

Color Measurement by Imaging Spectrometry

H. M. G. Stokman and Th. Gevers

Department of Intelligent Sensory Information Systems, Faculty of Science, University of Amsterdam, Kruislaan 403, 1098 SJ Amsterdam, Netherlands

E-mail: stokman@wins.uva.nl

and

J. J. Koenderink

Helmholtz Institute, University Utrecht, Netherlands

Received December 2, 1999; accepted April 26, 2000

Spectral imaging has the potential to make spatially resolved absolute color measurement possible for automatic visual inspection in industrial production applications. In this paper, a detailed description and evaluation of the calibration of such an imaging spectrograph is given. The reproducibility of the reflectance factors measured by the spectrograph is determined empirically and the measurements are compared to those of a spectrophotometer. Based on the CCD camera sensitivity, the probability that a measured color is within one CIE $L^*a^*b^*$ unit of the actual color is predicted theoretically. This result is verified in practice. © 2000 Academic Press

Key Words: visual inspection; imaging spectrometry; color measurement; error propagation; calibration.

1. INTRODUCTION

Automatic visual inspection of colors in an industrial production process can improve the overall quality of the product and is therefore of commercial interest. The advantage of computerized visual inspection over inspection by humans is that machines can evaluate color continuously and objectively. The inspection of spectra may also provide the possibility to trace the cause of an occurring color error. It is known that the amount of reflected light per wavelength can be measured by spectrophotometers with high precision. However, the disadvantage of the use of a spectrophotometer is that a color measurement application might require a higher spatial resolution than the minimal spatial resolution possible with a spectrophotometer. RGB color cameras do not suffer these drawbacks but are limited in the number of reflection factors that they can record (only three) from a test sample.

Over the past few years, new imaging sensors have become available. Optical Insights Ltd. recently introduced the MultiSpec Imager. The device is placed in front of a monochrome CCD camera and contains four different color filters. Four different filtered 2-D images are then projected onto the (monochrome) CCD grid. Further, Spectral Imaging Ltd. introduced the Inspector V7 spectrograph, which transforms the monochrome CCD camera into a line scanner: One axis displays the spatial information, whereas along the other axis the visible wavelength range is displayed. In this paper we investigate color measurement using the Inspector V7 spectrograph.

To our knowledge, no machine vision system exists today that is able to measure, at a large number of wavelengths, the amount of light reflected from a test sample and that is also able to compare this to the light reflected by a calibrated working standard (absolute color measurement). However, with a spectrograph such measurement of spectra becomes possible for industrial applications. The Inspector User's Manual [8] describes how to assemble and calibrate the spectrograph. The SpecLab User's Manual [9] describes the spectral imaging software provided with the spectrograph. Both manuals give basic directions for the calibration of the spectrograph. Finally, the application note 4 [7] gives a detailed description of calibration for absolute color measurement. However, no results are reported on the achievable precision of the measurement of spectra, for instance compared to other spectral measurement devices.

The contribution of this paper is that the obtainable accuracy of color measurement by a spectrograph is established. Test samples from the MacBeth ColorChecker are used, which is a checkerboard array of 24 colored squares in a wide range of colors. The measurement precision is determined empirically according to three criteria: (1) The short-term reproducibility, (2) the long-term reproducibility, and (3) absolute color measurement.

For industrial inspection, the CIE $L^*a^*b^*$ color space has been used extensively because it is approximately perceptual uniform. Two colors can be compared and the inspected color can be accepted or rejected based on the Euclidean distance between the colors in the CIE $L^*a^*b^*$ metric. For industrial applications, the spectra measured by spectral imaging would typically be transformed into the CIE $L^*a^*b^*$ color space. However, all measurements are subject to uncertainties. Burns and Berns [1] analyze the error propagation from a measured color signal to the CIE $L^*a^*b^*$ color space. The analysis indicates how the color space transform influences the mean, variance, and covariance of the colors under the influence of noise. Shafarenko *et al.* [5] use an adaptive filter for noise reduction in the CIE $L^*u^*v^*$ space prior to 3-D color histogram construction. The filter width depends on the covariance matrix of the noise distribution in the CIE $L^*u^*v^*$ space. Using the filter, the authors improve the segmentation results. Sharma and Trussell [6] describe a figure of merit used for the design and evaluation of color scanners and cameras. The advantage of the proposed measure is that it is based on error metrics in the CIE $L^*a^*b^*$ color space and also accounts for the varying noise performance of different filters.

For spectral imaging with a scientific grade CCD camera, the measurement uncertainties are caused by photon noise. Therefore, the second contribution of this paper is the proposal of a model predicting the propagation of photon noise to the color difference in CIE $L^*a^*b^*$ units between the observed and specified color. Using the photon noise model, it is investigated in theory how the noise affects the CIE XYZ values and CIE $L^*a^*b^*$ values. The result we aim for is the CIE $L^*a^*b^*$ value of a pixel with an expression of the reliability of the value. The main advantage for industrial inspection is that the predicted uncertainty is

available for the decision of what action needs to be taken if the measured color difference exceeds a predefined threshold.

This paper is organized as follows: In Section 2, a calibration model for the spectrograph and monochrome CCD camera configuration is presented. The calibration enables the theoretical propagation of the uncertainties of measured gray values to color differences. The error propagation due to measurement uncertainties of a spectrum to uncertainty in CIE $L^*a^*b^*$ units is then analyzed in Section 3. In Section 4, experimental results are presented, and a summary is given in Section 5.

2. CALIBRATION MODEL FOR THE SPECTROGRAPH

In this section, a calibration model for the spectrograph and monochrome CCD camera configuration is presented. The overall system diagram is shown in Fig. 1. A more detailed diagram of the spectrograph is given in Fig. 2.

Spectral smoothing. In this paper, the Jain CV-M300 camera is used with 576 pixels along the optical axis. We use the Inspector V7 spectrograph with shortest observable wavelength of 410 nm and longest wavelength of 705 nm. Setting the wavelength interval to 5 nm, the number of spectral samples obtained is 59. The pixels at position (x, y) of image h can therefore be averaged in spectral direction by a uniform filter of odd size $K = \lfloor 576/59 \rfloor$. If the pixel corresponding to wavelength λ is denoted as y_λ then the averaged spectral image h' is

$$h'(x, \lambda) = \frac{1}{K} \sum_{i=y_\lambda-K/2}^{y_\lambda+K/2} h(x, y_i) \quad (1)$$

although other methods of smoothing could also be used.

Equal-energy illumination calibration. The observed spectrum of a sample depends on the color of the illuminant, commonly modeled as

$$c(x, \lambda) = \int_{\lambda} f(\lambda) E(x, \lambda) R(x, \lambda) d\lambda, \quad (2)$$

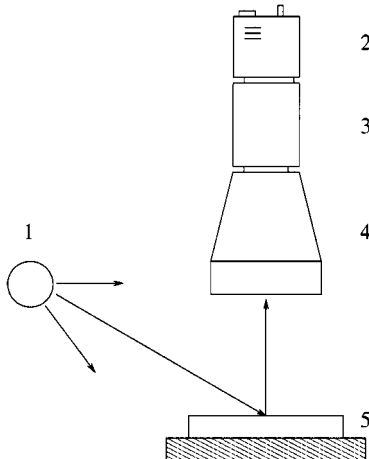


FIG. 1. Overall system diagram of the spectrograph and CCD camera configuration. Label (1) represents the light source, (2) the CCD camera, (3) the spectrograph, (4) the camera zoom lens, and (5) the object.

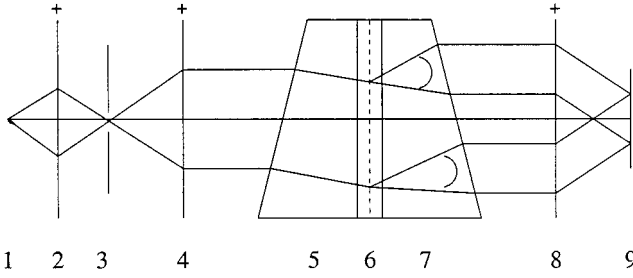


FIG. 2. Diagram of camera lens, spectrograph, and CCD camera configuration. Consider the point light source at (1). The light beam enters the camera lens (2), the spectrograph pinhole (3), and the spectrograph collimator lens (4). The light beam is dispersed into a range of wavelengths at the prism (5), grating (6), and prism (7) combination and enters the second spectrograph lens (8). The range of wavelengths is then projected onto the CCD detector array (9). The extension of the 1-D diagram to a 2-D diagram transforms the point light source (1) into a line light source. The vertical axis of the CCD detector records the spectral information, whereas the horizontal axis records the spatial information.

where $c(x, \lambda)$ is the observed sensor value at position x , $f(\lambda)$ is the transmission of a filter, $E(x, \lambda)$ is the spectral distribution of the irradiance per wavelength λ at position x , and $R(x, \lambda)$ is the spectral albedo of the object R at that position. In this paper, the interest is in the spectrum $R(\lambda)$ independent of the color of the illuminant. The reflectance of a matte uniform colored white reference sample with response $R_w(\lambda)$ is given by

$$w(x, \lambda) = \int_{\lambda} f_n(\lambda) E(x, \lambda) R_w(\lambda) d\lambda. \tag{3}$$

Correction of a spectral image $c(x, \lambda)$ taken from a test sample by the white reference image gives

$$\frac{c(x, \lambda)}{w(x, \lambda)} = \frac{\int_{\lambda} f(\lambda) E(x, \lambda) R_c(x, \lambda) d\lambda}{\int_{\lambda} f(\lambda) E(x, \lambda) R_w(\lambda) d\lambda} = \frac{R_c(x, \lambda)}{R_w(\lambda)} \tag{4}$$

assuming that the filter $f(\lambda)$ is a narrow band filter modeled as a unit impulse. Equation (4) implies that the observed spectra are independent of the actual spectral distribution of the light source and the spatial variance of the intensity of the illuminant. As $R_w(\lambda)$ is known from a calibrated standard then

$$R_c(x, \lambda) = \frac{c(x, \lambda)}{w(x, \lambda)} \cdot R_w(\lambda) \tag{5}$$

gives the true fraction of reflected light by the sample.

3. ERROR PROPAGATION

For industrial inspection, the CIE $L^*a^*b^*$ color space is important because it is approximately perceptually uniform. The inspected color can be accepted or rejected based on the Euclidean distance in the CIE $L^*a^*b^*$ metric. A just noticeable color difference corresponds to one CIE $L^*a^*b^*$ unit. However, all measurements are subject to some uncertainty. For spectral imaging with a scientific grade camera, the uncertainties are caused by photon

noise. In this section, a model is developed predicting how photon noise affects the uncertainty in a color difference as measured. The result we aim for is the CIE $L^*a^*b^*$ value of a pixel with an expression of the reliability of the value. The main advantage for industrial inspection is that the predicted uncertainty is available for the decision of what action needs to be taken if the measured color difference exceeds a predefined threshold.

3.1. Equations for Error Propagation

The result of a measurement of a quantity x is stated as

$$\hat{x} = x_{\text{est}} \pm \delta x, \quad (6)$$

where x_{est} is the estimate for the quantity x (e.g., the average value) and δx is the uncertainty in the measurement of x (e.g., the standard deviation). Suppose that x, \dots, z are measured with corresponding uncertainties $\delta x, \dots, \delta z$; then the uncertainty in function $q(x, \dots, z)$ is [10]

$$\delta q = \sqrt{\left(\frac{\partial q}{\partial x} \delta x\right)^2 + \dots + \left(\frac{\partial q}{\partial z} \delta z\right)^2} \quad (7)$$

if and only if the uncertainties $\delta x, \dots, \delta z$ are relatively small, independent, and random. $\partial q / \partial x, \dots, \partial q / \partial z$ denote the partial derivatives of q with respect to x, \dots, z . In any case, the uncertainty in q is never larger than the ordinary sum

$$\delta q \leq \left| \frac{\partial q}{\partial x} \right| \delta x + \dots + \left| \frac{\partial q}{\partial z} \right| \delta z \quad (8)$$

iff the uncertainties $\delta x, \dots, \delta z$ are relatively small. These two equations will be used in the next section to propagate uncertainties.

3.2. Propagation of Uncertainties due to Photon Noise

We use a polynomial camera model

$$h(x, y) = g \cdot f(x, y), \quad (9)$$

where f is the input signal, g denotes the gain, and h is the output signal. Modern CCD cameras are sensitive enough to count individual photons. Photon noise arises from the fundamentally stochastic nature of photon production. The probability distribution for counting ρ photons during t seconds is known to be Poisson. For a Poisson distribution, the number of photons measured by an image sensing element at position (x, y) is given by its average as

$$\hat{f}(x, y) = \rho t \pm \sqrt{\rho t}, \quad (10)$$

where ρ is the rate of photons measured per second. When the average number of counts is large the Poisson distribution is approximated well by the Gauss distribution around mean value \hat{f} with standard deviation $\delta_f = \sqrt{\hat{f}}$.

Our aim is to analyze how uncertainty $\delta f(x, y)$ propagates to the uncertainty in a color difference. Consider the camera model described in Eq. (9). The number of electrons, or sensitivity S , necessary to change between two subsequent levels of brightness is given by van Vliet *et al.* [3] as

$$S = 1/g. \quad (11)$$

Sensitivity can be measured by substitution of Eq. (10) in Eq. (9):

$$\hat{h}(x, y) = g \cdot (\rho t \pm \sqrt{\rho t}). \quad (12)$$

Using $\hat{h} = g \cdot \rho t$ and standard deviation $\delta h = g \cdot \sqrt{\rho t}$ of a region with homogeneous pixel values, the sensitivity S for a particular CCD camera is derived as

$$S = \frac{\hat{h}}{(\delta h)^2}. \quad (13)$$

From Eqs. (12) and (13) it follows that the uncertainty in the number of photons measured at an arbitrary pixel $g(x, y)$ is given by

$$\delta g(x, y) = \sqrt{\frac{\hat{h}(x, y)}{S}}. \quad (14)$$

After the smoothing operation (Eq. (1)), the uncertainty reduces to the standard deviation of the mean,

$$\delta g(x, \lambda) = \frac{\delta g(x, y)}{\sqrt{K}}, \quad (15)$$

and from Eq. (5) it follows that the uncertainty in the reflectance percentage is

$$\delta R(x, \lambda) = R_w(x, \lambda) \sqrt{\frac{c(x, \lambda)^2 \delta w(x, \lambda)^2}{w(x, \lambda)^4} + \frac{\delta c(x, \lambda)^2}{w(x, \lambda)^2}}. \quad (16)$$

The CIE XYZ values are computed from the reflectance percentage $R(x, \lambda)$ as [11]

$$X(x) = \frac{100}{k} \sum S(\lambda) R(x, \lambda) \bar{x}(\lambda) \quad (17)$$

$$Y(x) = \frac{100}{k} \sum S(\lambda) R(x, \lambda) \bar{y}(\lambda) \quad (18)$$

$$Z(x) = \frac{100}{k} \sum S(\lambda) R(x, \lambda) \bar{z}(\lambda), \quad (19)$$

where $S(\lambda)$ is the CIE standard illuminant and \bar{x} , \bar{y} , \bar{z} the color-matching functions of a CIE standard observer. k is a normalization factor computed from Eq. (18) by substitution of the perfect diffuser for $R(\lambda)$. Using the CIE formulae, the uncertainty in the XYZ values

at position x is

$$\delta X(x) = \frac{100}{k} \sum_{\lambda} S(\lambda) \delta R(x, \lambda) \bar{x}(\lambda) \quad (20)$$

$$\delta Y(x) = \frac{100}{k} \sum_{\lambda} S(\lambda) \delta R(x, \lambda) \bar{y}(\lambda) \quad (21)$$

$$\delta Z(x) = \frac{100}{k} \sum_{\lambda} S(\lambda) \delta R(x, \lambda) \bar{z}(\lambda). \quad (22)$$

From the XYZ coordinates, the CIE $L^*a^*b^*$ coordinates are computed as

$$L^*(x) = \begin{cases} 116 \left(\frac{Y(x)}{Y_n} \right)^{1/3} - 16 & \text{if } \frac{Y(x)}{Y_n} > 0.008856 \\ 903.3 \left(\frac{Y(x)}{Y_n} \right) & \text{otherwise} \end{cases} \quad (23)$$

$$a^*(x) = 500 \left[f \left(\frac{X(x)}{X_n} \right) - f \left(\frac{Y(x)}{Y_n} \right) \right] \quad (24)$$

$$b^*(x) = 200 \left[f \left(\frac{Y(x)}{Y_n} \right) - f \left(\frac{Z(x)}{Z_n} \right) \right] \quad (25)$$

$$f(s) = \begin{cases} (s)^{1/3} & \text{if } s > 0.00856 \\ 7.787(s) + \frac{16}{116} & \text{otherwise,} \end{cases} \quad (26)$$

where $X_n Y_n Z_n$ is the reference white point. In this paper, it is assumed that all samples have a reflection such that the low lighting conditions (the “otherwise” cases) of Eqs. (23)–(26) can be ignored. From Eq. (8) it follows that the uncertainty δL^* at position x is

$$\delta L^*(x) = \left| \frac{116}{3 \left(\frac{Y(x)}{Y_n} \right)^{2/3} Y_n} \right| \delta Y(x). \quad (27)$$

However, for the uncertainties δa^* and δb^* , the XYZ values are dependent due to overlapping color matching functions $\bar{x}(\lambda)$, $\bar{y}(\lambda)$, $\bar{z}(\lambda)$. Therefore, Eq. (8) is used to establish that

$$\delta a^*(x) \leq \left| \frac{500}{3 \left(\frac{X(x)}{X_n} \right)^{2/3} X_n} \right| \delta X(x) + \left| \frac{500}{3 \left(\frac{Y(x)}{Y_n} \right)^{2/3} Y_n} \right| \delta Y(x) \quad (28)$$

$$\delta b^*(x) \leq \left| \frac{200}{3 \left(\frac{Y(x)}{Y_n} \right)^{2/3} Y_n} \right| \delta Y(x) + \left| \frac{200}{3 \left(\frac{Z(x)}{Z_n} \right)^{2/3} Z_n} \right| \delta Z(x). \quad (29)$$

The CIE 1976 color difference formula is

$$\Delta E^*(x) = \sqrt{(\Delta L^*(x))^2 + (\Delta a^*(x))^2 + (\Delta b^*(x))^2}, \quad (30)$$

where $\Delta L^*(x)$, $\Delta a^*(x)$, $\Delta b^*(x)$ are the differences between the CIE $L^*a^*b^*$ values at

position x . If CIE $L^*a^*b^*$ values are compared to target CIE $L^*a^*b^*$ values which have no associated uncertainties, then the uncertainty in the color difference ΔE^* between the target and measured values follows from Eq. (8) as

$$\delta E^*(x) \leq \frac{|\Delta L^*(x)|\delta L^*(x) + |\Delta a^*(x)|\delta a^*(x) + |\Delta b^*(x)|\delta b^*(x)}{\sqrt{(\Delta L^*(x))^2 + (\Delta a^*(x))^2 + (\Delta b^*(x))^2}}. \quad (31)$$

In industrial inspection, a measured color will be compared to a reference color, and these colors should be the same unless an error occurred in the production process. The question of interest then is what the probability is that the measured color falls within one CIE $L^*a^*b^*$ unit of this reference color. As the predicted δE^* is approximately known, the probability that the measured color falls within one CIE $L^*a^*b^*$ unit of the reference color is

$$P(\Delta E^* < 1) = \text{erf}(1/\delta E^*), \quad (32)$$

where $\text{erf}()$ is the commonly known normal error integral transforming the standard deviation into probability assuming a Gaussian distribution of the uncertainties.

4. EXPERIMENTS

Unless stated otherwise, all experiments are performed using a Jain CV-M300 monochrome CCD camera, Matrox Corona Frame-grabber, Navitar 7000 zoom lens, and Imspecor V7 spectrograph. Further, a Spectalon white reference [2], 500 W halogen illumination, and the MacBeth ColorChecker are used for the experiments. CIE $L^*a^*b^*$ values are stated for Standard Illuminant A and the CIE 1931 Standard Observer for 5-nm intervals [11]. The missing values at the two ends of the spectrum are set equal to the nearest measured reflectance factors. The spatial resolution is 40 μm per pixel and the exposure time of the 8-bits camera is 1/25 s per frame.

In Section 4.1, the calibration of the spectrograph is described. In Section 4.2, experiments are described that check the validity of the proposed model to predict the propagation of photon noise to a measured color difference. Finally, the accuracy of color measurement by a spectrograph is established in Section 4.3.

4.1. Calibration

The following experiments check or adjust the spectrograph output by comparison with calibrated standards in order to determine the true values of the fraction of reflected light.

Photometric scale calibration. The camera lens is covered with a dark sheet which contains a small hole with radius of approximately 0.5 cm. Two halogen light sources are used to illuminate the white reference. Three recordings of the white reference are made: One recording when the white reference is illuminated by one illuminant, the second recording when the reference is illuminated by the second illuminant, and the third recording using both illuminants. Invariably, the three recordings show a small, bright circle with varying intensity. The average brightness value is computed over the circle for the three images over $N \approx 15,000$ pixels. The values are 104 ± 4 , 123 ± 4 for the two singly illuminated circles, and 219 ± 6 for the doubly illuminated circle, respectively. The dark current is measured as 6 ± 1 in the scale of $0 \cdots 255$. After correction for the dark current, the discrepancy is less than one percent and it is concluded that the camera output is linear.

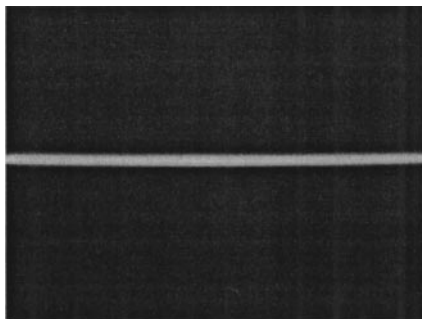


FIG. 3. Multispectral image of a white sample using Orion filter s10_550s. A horizontal line is observed in the image. The precise row at the optical axis that corresponds to the bandpass wavelength is detected through convolution with a one-dimensional Gauss filter.

Wavelength calibration. For the experiment, narrow bandpass filters are used which transmit at 50-nm intervals in the visible wavelength range. They have a transmittance of 10-nm bandwidth around their bandpass wavelength [4]. The filters are placed in front of the camera lens and an image is captured of a white sample. The aperture is adjusted for each filter to obtain a maximal signal; see Fig. 3. The position at the optical axis of the line corresponds to the transmitted wavelength of the filter. A low sensitivity of the CCD camera is seen for lower wavelengths. Estimation of the bandpass wavelength is done by convolution with a one-dimensional Gauss filter with $\sigma = 10$ pixels. The results are averaged over the spatial axis and are given in Table 1. The rows corresponding to 5-nm intervals are obtained by linear interpolation from the results. The table shows that the minimal distance between two consecutive (50 nm apart) bandpass filters is 89.3 pixels. Our interest is in a spectral resolution of 5 nm. The width of the filter of Eq. (1) is therefore $K = 89.3/10 = 9$ pixels sufficient for our purposes.

4.2. Propagation of Uncertainties from Photon Noise to Color Differences

In this section, the model of Section 3.2 predicting how photon noise affects the uncertainty in a measured color difference is verified empirically.

Establishing sensitivity parameter S . For this experiment, the Jain camera with zoom lens is used, the Dolan & Jenner fiber optic diffuse axial illuminator AI-2, Dolan & Jenner light source PL-800, and the Spectralon white reference. The aperture is gradually reduced in seven steps, thus reducing the amount of incoming light in the CCD camera. The precision

TABLE 1
Optical Axis Calibration

λ (nm)	\bar{y}
450	90.59 ± 0.05
500	192.20 ± 0.05
550	281.73 ± 0.04
600	378.20 ± 0.04
650	470.40 ± 0.04
700	559.71 ± 0.03

TABLE 2
Establishing Sensitivity Parameter S

\bar{f}	$S = \bar{f}/\sigma^2$
179.8 ± 3.4	17.5
147.0 ± 3.2	16.0
131.6 ± 2.9	18.3
114.4 ± 2.7	18.2
88.1 ± 2.4	20.4
76.1 ± 2.2	21.7
50.4 ± 1.9	22.6
	19.2 ± 2.4

of the obtained value of S depends on the ability to obtain an image patch with constant gray values. To that end, a diffuse illuminator is used, combined with manual selection of a sub-region in the image. The observed average pixel value and standard deviations of the images are given in Table 2. The experiment shows that, given the integration time and intensity of the illumination, the sensitivity of the camera described in Eq. (11) approximates 19 ± 2 .

Propagation of uncertainties. For the experiment, the spectral image from the white patch 19 of the MacBeth ColorChecker is taken. Models were proposed in Section 3.2 to predict the propagation of uncertainties from photon noise to uncertainty in CIE $L^*a^*b^*$ values. The goal of this experiment is to analyze the validity of the developed formulae.

In the previous experiment the sensitivity parameter S is determined. In the current experiment, the uncertainty in $R(x, \lambda)$, $XYZ(x)$, and CIE $L^*a^*b^*(x)$ values is predicted using S . The predicted uncertainties are then averaged over the spatial range. The actual uncertainty is derived from the standard deviation of $R(x, \lambda)$, $XYZ(x)$, and CIE $L^*a^*b^*(x)$ values over the spatial range.

First, the predicted and actual uncertainties in the reflection percentage are compared. These uncertainties per wavelength are shown in Fig. 4. The absolute difference between

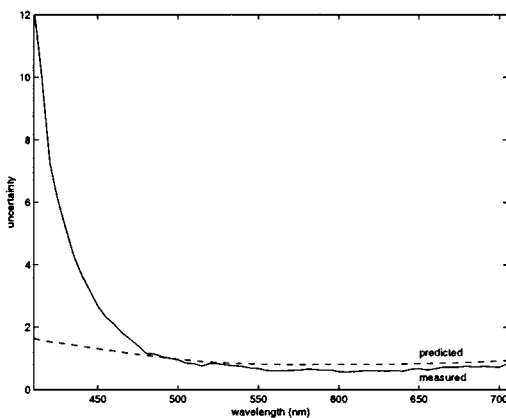


FIG. 4. Experiment: Comparison of the predicted (dashed line) versus the actual uncertainty (solid line) of the reflection percentages. The absolute difference averaged over the wavelength range is $1 \pm 2\%$. Except for the short wavelengths, where the computation of $R(\lambda)$ is unstable due to the low sensitivity of the CCD camera and low transmittance of the illuminant at short wavelengths, the figure shows a reasonable correspondence between the predicted and actual uncertainty.

TABLE 3
Comparison of Predicted vs Measured Uncertainties in XYZ,
CIE $L^*a^*b^*$ and ΔE Values

	δX	δY	δZ	δL^*	δa^*	δb^*	δE^*
Predicted	0.8	0.7	0.5	0.3	2.6	1.6	2.2
Measured	0.9	0.9	0.4	0.4	0.3	0.5	0.6

the actual and the predicted error averaged over the wavelength range is 1 ± 2 . Except for the short wavelengths, where the computation of $R(\lambda)$ is unstable due to the low sensitivity of the CCD camera and low transmittance of the illuminant at short wavelengths, the figure shows a reasonable correspondence between the predicted and actual uncertainty.

Second, the predicted and actual uncertainties in the XYZ values are compared in Table 3. The table shows a close correspondence between the predicted and actual values. Third, the predicted and actual uncertainty in the CIE $L^*a^*b^*$ values are also compared in Table 3. The predicted and actual uncertainties in the L^* value correspond closely. In contrast, the predicted uncertainties in the a^* , b^* value are overestimations of the actual uncertainties. This can be understood from Eqs. (28) and (29): The uncertainty in δa^* depends on the overlapping color matching functions \bar{x} and \bar{y} . Therefore uncertainties δX and δY are interdependent and as a result the uncertainty in a^* is overestimated. Consequently, the uncertainty in ΔE^* is overestimated as well. Still, the predicted values correspond to the uncertainty model of Eq. (8): For dependent variables, the actual uncertainty should be less than or equal to the predicted uncertainty.

The experiment shows that the proposed theoretical model for prediction of uncertainty due to photon noise to the uncertainty in the reflection percentage, the XYZ , and CIE $L^*a^*b^*$ values gives reasonable predictions of the actual uncertainties.

4.3. Accuracy of Color Measurement

The accuracy of color measurement by spectrograph is empirically established by the following experiments:

Short-term reproducibility. For the experiment, 10 spectral images are taken of the white patch 19 of the MacBeth ColorChecker. The only difference between the images is that they are recorded a few seconds apart. Goal of the experiment is to examine the short-term reproducibility. Compared to the first image, the average difference in the reflection percentage $\overline{\%R} = 0.3 \pm 0.3$. The experiment shows that the error in the short-term reproducibility is less than 1% assuming that the average difference in the reflection percentage is normally distributed.

Long-term reproducibility. For the experiment, the 24 patches of the MacBeth ColorChecker are recorded twice. The difference between the two image sets is that between the two recordings the camera, spectrograph, and illuminant setup were disassembled and restored one week later. The goal of the experiment is to examine the long-term reproducibility of the output of the spectrograph. The average reflection percentage difference between the two spectral image sets is $\overline{\%R} = 1.6 \pm 1.5$. Differences are caused by the errors due to the short-term reproducibility and by minor differences in the image

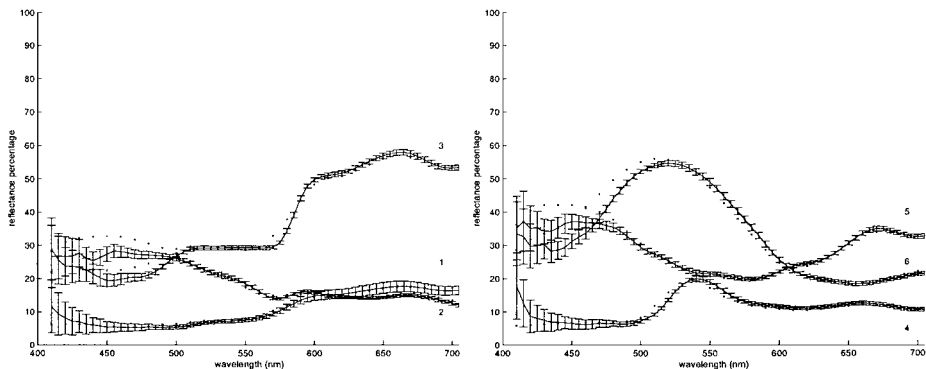


FIG. 5. Experiment: Comparison of the spectrograph with a spectrophotometer. Left: Color patches 1 (dark skin), 2 (light skin), and 3 (blue sky). Right: Color patches 4 (foliage), 5 (blue flower), and 6 (bluish green). Error bars denote the standard deviation of the average reflectance percentage measured by the Imspector V7 spectrograph. Dotted lines denote the reflectance percentage measured by X-Rite SP78 spectrophotometer.

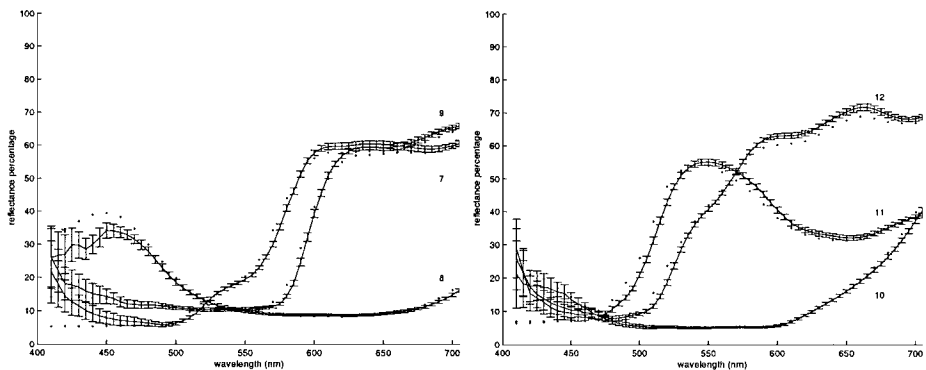


FIG. 6. Experiment: Comparison of the spectrograph (error bars) with a spectrophotometer (dots). Left: Color patches 7 (orange), 8 (purplish blue), and 9 (moderate red). Right: Color patches 10 (purple), 11 (yellow green), and 12 (orange yellow).

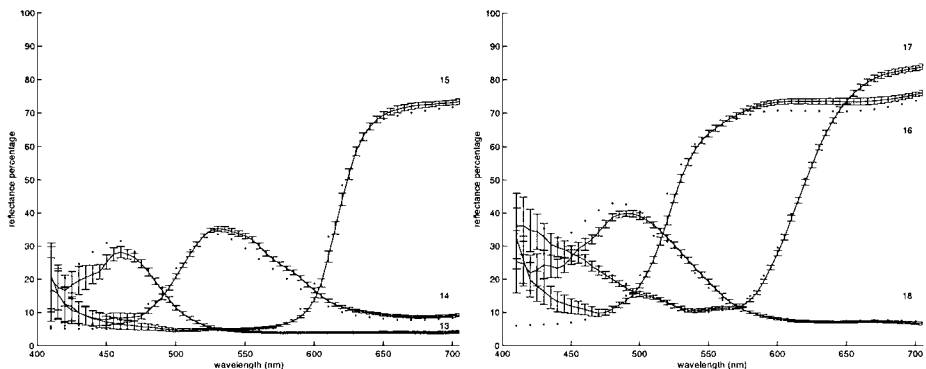


FIG. 7. Experiment: Comparison of the spectrograph (error bars) with a spectrophotometer (dots). Left: Color patches 13 (blue), 14 (green), and 15 (red). Right: Color patches 16 (yellow), 17 (magenta), and 18 (cyan).

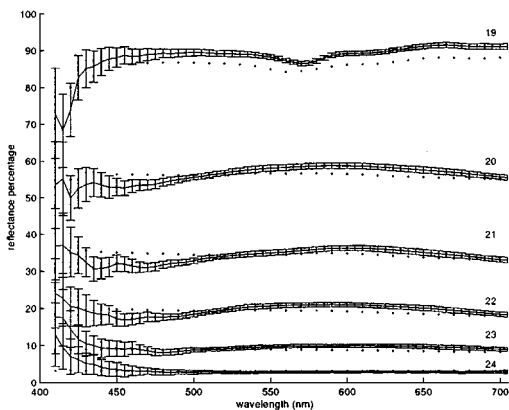


FIG. 8. Experiment: Comparison of the spectrograph (error bars) with a spectrophotometer (dots). Color patches 19 (white) to 24 (black).

acquisition setup. The experiment shows that the error in the long-term reproducibility is less than 5%.

Comparison of the spectrograph with a spectrophotometer. For this experiment, the MacBeth ColorChecker, the Jain camera and Imspector V7, and a X-Rite SP78 Sphere Spectrophotometer are used. The spectrophotometer samples the visible wavelength at 10-nm intervals. The goal of the experiment is to compare the reflectance percentages measured by the spectrograph with that of the spectrophotometer. The reflectances that are compared are in the range of 410 ··· 700 nm; the wavelength interval is 10 nm. The differences in reflectances are shown in Figs. 5–8. The average difference in the reflection percentage is $\%R = 2.0 \pm 0.7$. The experiment shows that the difference in reflectance percentage between the spectrograph and a spectrophotometer is less than 5%.

5. DISCUSSION

The cost of the spectrograph, CCD camera and frame-grabber, calibration white reference tile, and narrow bandpass filters is comparable to that of a spectrophotometer. Compared to the spectrophotometer, the spectrograph gives a higher spectral resolution and arbitrary spatial resolution and can measure the spectral distribution of a color without making contact with the sample. The required exposure time (1/25 s) is shorter than that of a spectrophotometer.

This paper gives a detailed description of the calibration of the Imspector V7. The error in short-term reproducibility of the reflectance percentage is less than 1%. The error in long-term reproducibility is less than 5%. Comparison of the spectrograph with a spectrophotometer gives a difference in the reflectance percentage less than 5%. These results could further be improved if, e.g., the temporal variation of the illumination could be kept constant, and by, e.g., using more sophisticated filtering methods along the spectral direction of the image.

A model was proposed which predicts the probability that a measured color is within one CIE $L^*a^*b^*$ unit of the actual color based on the camera sensitivity. The theoretical result was verified in practice. The result is important for an automated color inspection system:

The predicted uncertainty is available for the decision of what action needs to be taken if a measured color difference exceeds a predefined threshold.

REFERENCES

1. P. D. Burns and R. S. Berns, Error propagation analysis in color measurement and imaging, *Color Research Appl.* **22**(4), 1997, 280–289.
2. Labsphere Inc., Reflectance Calibration Laboratory, *Calibration Certificate*, Spectralon Reflectance Target, Sample I.D.: SRT-99-050, September 1998.
3. J. C. Mullikin, L. J. van Vliet, H. Netten, F. R. Boddeke, G. van der Feltz, and I. T. Young, Methods for ccd camera characterization, in *Image Acquisition and Scientific Imaging Systems* (H. C. Titus and A. Waks, Eds.), Vol. 2173, pp. 73–84, SPIE, Philadelphia, 1994.
4. Orion Corp., Technical Data, Filters s10_400s, s10_450s, s10_500s, s10_550s, s10_600s, s10_650s, s10_700s, October 1998.
5. L. Shafarenko, M. Petrou, and J. Kittler, Histogram-based segmentation in a perceptually uniform color space, *IEEE Trans. Image Process.* **7**, 1998, 1354–1358.
6. G. Sharma and H. Joel Trussell, Figures of merit for color scanners, *IEEE Trans. Image Process.* **6**, 1997, 990–1001.
7. Spectral Imaging Ltd., *Data Processing in Precise Spectral Imaging*, 1997.
8. Spectral Imaging Ltd., *ImSpector Imaging Spectrograph User Manual Version 1.7*, 1997.
9. Spectral Imaging Ltd., *SpecLab User Manual Version 1.3*, 1998.
10. J. R. Taylor, *An Introduction to Error Analysis*, University Science Books, Mill Valley, CA, 1982.
11. G. Wyszecki and W. S. Stiles, *Color Science: Concepts and Methods, Quantitative Data and Formulae*, 2nd ed., Wiley, New York, 1982.